J. Earth Planet. Sci. Nagoya Univ., Vol. 51, 11 to 35, 2004

Rare earth element and Sr isotopic study of the Middle Permian limestone-dolostone sequence in Kuzuu area, central Japan: Seawater tetrad effect and Sr isotopic signatures of seamount-type carbonate rocks

Noriko MIURA, Yoshihiro ASAHARA and Iwao KAWABE*

Department of Earth and Planetary Sciences, Graduate School of Environmental Studies, Nagoya University, Chikusa, Nagoya 464-8602, Japan
(Received October 25, 2004 / Accepted December 29, 2004)

ABSTRACT

The Kuzuu limestone-dolostone complex, in central Japan, is a remnant of the Middle Permian carbonate succession formed on a basaltic seamount in an open-sea realm without inputs of terrigenous materials. REE and Sr isotopic data of the carbonate rocks are clues to understanding the diagenetic process of biogenic carbonates to form crystalline carbonate minerals. The $^{87}Sr/^{86}Sr$ ratios of bulk carbonate samples are 0.7073–0.7076, and their Sr isotopic stratigraphic age (260±5 Ma) coincides with their fusulinid fossil age (263±8 Ma). The carbonate rocks have much higher REE/Ca ratios than modern skeletal biogenic carbonates by factors of 10^2–10^4. Their REE/Ca ratios are about one order of magnitude higher than those of microbialite. The chondrite-normalized REE patterns for the Kuzuu samples show large negative Ce anomalies, together with seawater-like tetrad effects and high Y/Ho ratios. The Ce anomalies are comparable to those of present-day ocean waters at depths of 600–800 m, except for the bottom part samples polluted with Fe(III) oxyhydroxide possibly by fluids derived from underlying basaltic volcanics. Their REE patterns normalized by Pacific seawater at a depth of 381 m exhibit smooth light REE enrichment trends similar to the experimental partition coefficients of REE between calcite-overgrowths and seawater solutions. There is no significant difference in REE and Y features between the limestone and dolostone members. The original biogenic carbonates deposited on a basaltic seamount in shallow water environment, but subsequently they were subsided to the water depths suggested by their Ce anomalies. At the water depth, the biogenic carbonates were re-crystallized to calcite under a condition of sufficient supply of the seawater, and the seawater REE and Y were incorporated into calcite. The $^{87}Sr/^{86}Sr$ ratios of dolomite, however, are slightly lower than those of coexistent calcite by 0.0002, which is a time interval of about 2 Ma from the seawater $^{87}Sr/^{86}Sr$ curve for Middle to Late Permian. The dolomitization occurred almost immediately after the re-crystallization of biogenic carbonate to calcite in a moderately deep water, but did not alter the REE and Y features of limestone precursors. This is consistent with the recent diagenetic model for the carbonate sequences of Neogene atolls in the Pacific emphasizing the role of thermal convection of moderately deep water.

INTRODUCTION

Rare earth elements (REEs) in ancient marine limestones and associated dolostones

*The corresponding author (e-mail: kawabe@eps.nagoya-u.ac.jp)

have attracted much attention, because their REE signatures may provide insight not only into the depositional marine environments of carbonate formations but also into the diagenesis of sedimentary carbonates and dolomitization (Banner et al., 1988a; Kawabe et al., 1991; Qing and Mountjoy, 1994; Bellanca et al., 1997; Tanaka et al., 2003; Mazumdar et al., 2003). Distinctive REE signatures of ancient seawater probably comparable to those of present-day seawater (Piepgras and Jacobsen, 1992; German et al., 1995; Zhang and Nozaki, 1996; Kawabe et al., 1998) and its modification records by subsequent diagenesis may be retained in ancient marine carbonate rocks. In addition, radiogenic Sr and Nd isotopic compositions of ancient carbonate rocks have also been used in order to constraint diagenetic fluids and ancient seawater as well (Shaw and Wasserburg, 1985; Banner et al., 1988a, b; Mountjoy et al., 1992; Denison et al., 1994; Tanaka et al., 2003).

Although the marine carbonate rocks dealt with in these geochemical and isotopic studies are collectively called marine limestones or marine carbonate rocks, they must be divided into two main groups: the continental platform type (Banner et al., 1988a; Bellanca et al., 1997; Mazumdar et al., 2003) and the seamount-type (Kawabe et al., 1991; Tanaka et al., 2003). The continental platform carbonate rocks often contain impurities of non-carbonate materials of terrigenous origins as well as authigenic materials formed in coastal waters. Hence REEs in the continental platform carbonate rocks are sometimes enriched in non-carbonate impurities like Fe-oxyhydroxide (Shaw and Wasserburg, 1985). The Sr and Nd isotopic compositions of their bulk samples are also affected by such non-carbonate impurities (Denison et al., 1994; Shaw and Wasserburg, 1985). On the other hand, the seamount-type carbonate rocks, like those occurring on the tops of volcanic islands in the western Pacific, are less likely to be affected by terrigenous materials. The two types of marine carbonate rocks are quite different with respect to their qualities as "chemical and isotopic fossils of seawater". Coral reef carbonate rocks of the Late Paleozoic formed in open-sea realm are frequently found as exotic blocks in the Mesozoic accretionary terranes of Japanese Islands, and their fossil ages and stratigraphic studies are well-known (Sano and Kanmera, 1988). Majority of the carbonate rocks are of the seamount type, and scarcely have non-carbonate impurities. They are good samples of "chemical and isotopic fossils of seawater" in the geological past (Tanaka et al., 2003).

The limestone-dolostone associations are well known in Tertiary to Holocene atoll carbonate sequences in the Pacific. The limestone-dolostone associations in the Pacific atolls are the geological evidence for their diagenetic formations from biogenic carbonate sequences in reaction with fluids involving seawater. However, there has been intense debate about which type of fluid played the major role in the diagenesis: the roles of meteoric water (Rodgers et al., 1982), evaporated seawater (Schofield and Nelson, 1978; Ohde and Elderfield, 1992), and relatively deep seawater (Aharon et al., 1987; Flood et al., 1996) have been emphasized in the diagenetic formation of dolomite in atoll sequences.

This paper reports our REE and Sr isotopic study of the Middle Permian limestone-dolostone complex in Kuzuu area, Tochigi Prefecture, central Japan. This carbonate rock sequence, approximately 300 m thick, is called the Nabeyama Formation, and subdivided into the Lower Limestone, Middle Dolostone, and Upper Limestone mem-

bers (Matsuda and Iijima, 1989). They represent a significant part of a coral reef carbonate sequence of the Middle Permian emplaced tectonically in the Mesozoic accretionary complexes.

The content of non-carbonate impurities of the Kuzuu carbonate rocks is quite low: The average non-carbonate content is only 1% for the Upper Limestone and Middle Dolostone, and 2.6% for the Lower Limestone (Fujinuki et al., 1982). They are originally biogenic carbonate sediments deposited on a basaltic seamount in an open-sea environment least affected by terrigenous material inputs. Hence they are geologically similar to the Tertiary to Holocene atoll carbonate sequences in the Pacific, not to the continental platform-type carbonate sequences. We will focus our attention on how seawater REE and Sr isotopic signatures in Middle Permian are retained in the carbonate rocks and how REE and Sr isotopic features are different between the limestones and dolostones.

KUZUU CARBONATE SEQUENCE FORMED ON A BASALTIC SEAMOUNT

In the Kuzuu area (Fig. 1-a), the Permian, Triassic and Jurassic strata occur as thrust sheets making an imbricate structure, and the thrust sheets are grouped into the carbonate-dominated and chert-dominated ones (Matsuda and Iijima, 1989). The limestone-dolostone sequence (the Nabeyama Formation) occurs as a main constituent of the carbonate-dominated thrust sheets. The Nabeyama formation with thickness of about 300 m consists of the Lower Limestone, Middle Dolostone, and Upper Limestone members as noted above. The Lower and Upper Limestones yield abundant *Parafusunina* and the other Middle Permian fusulinids. This limestone-dolostone sequence conformably overlies submarine mafic pyroclastic rocks and lavas called the Izuru Formation with thickness of about 500 m (Fig. 1-b). Perhaps the original thickness was more than 500 m, although the bottom of the Izuru Formation is cut by thrust faults (Yanagimoto, 1973; Kobayashi, 1979; Matsuda and Iijima, 1989). The upper part of the Izuru Formation intercalates lenticular limestones and thin calcareous layers, from which fusulinid fossils of the Middle Permian *Parafusulina* zone have been reported (Kobayashi, 1979). Geologic ages of both the upper part of the Izuru Formation and Nabeyama Formation are the Middle Permian.

The Nabeyama limestone-dolostone sequence is unconformably overlain by the Nagaami Formation composed of calcirudites with limestone rubbles and laminated limestones (Matsuda and Iijima, 1989). The Nagaami Formation covers and fills karstified surface structures of carbonate rocks of the Nabeyama Formation. The limestone rubbles contain not only fusulinid fossils of the Middle Permian *Parafusulina* zone but also the Upper Permian fusulinids of *Neoschwagerina*, *Yabeina*, *Codonofusiella-Reichelina* and *Palaeofusulina-Reichelina* zones (Igo and Igo, 1977), but no fossil of the Triassic has been reported. In contrast, a mixed conodont assemblage found in the laminated limestones and matrices of the calcirudites of the Nagaami Formation, indicates a wide range of fossil ages from the Middle Permian to the Upper Triassic (Igo and Igo, 1977; Kobayashi, 1979; Matsuda and Iijima, 1989). The calcirudites with limestone rubbles of the Nagaami Formation by Matsuda and Iijima (1989) are described as the basal conglomerates of the Upper Triassic Adoyama Formation of

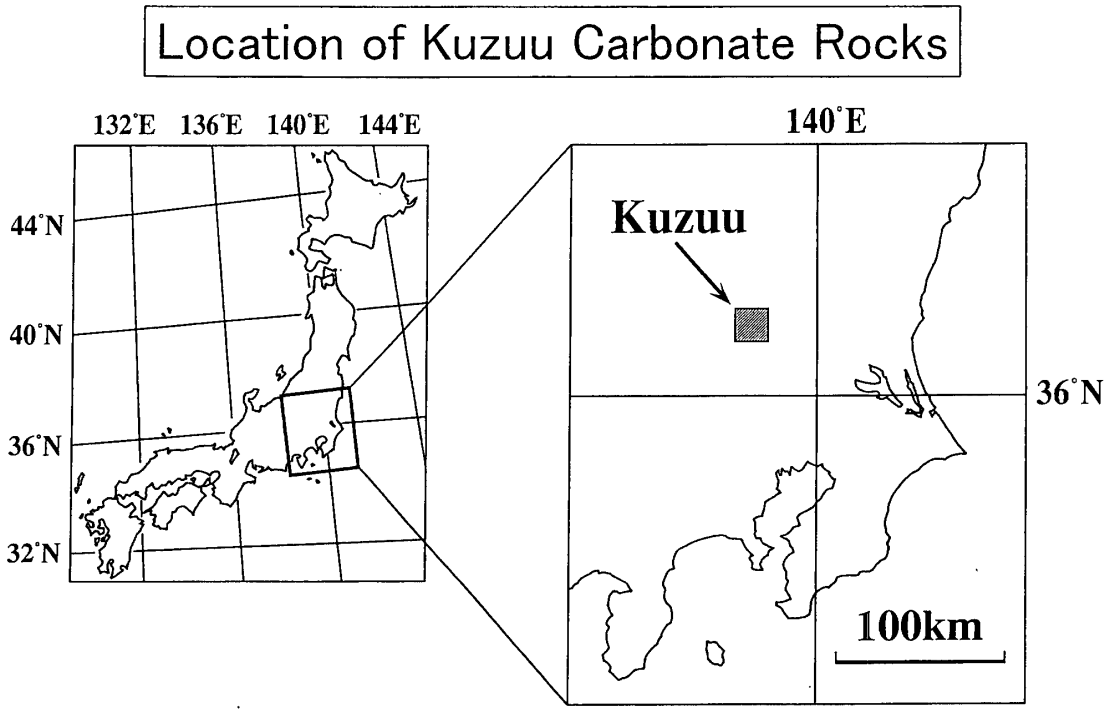

Fig. 1-a. The location of Kuzuu limestone-dolostone complex (Nabeyama Formation).

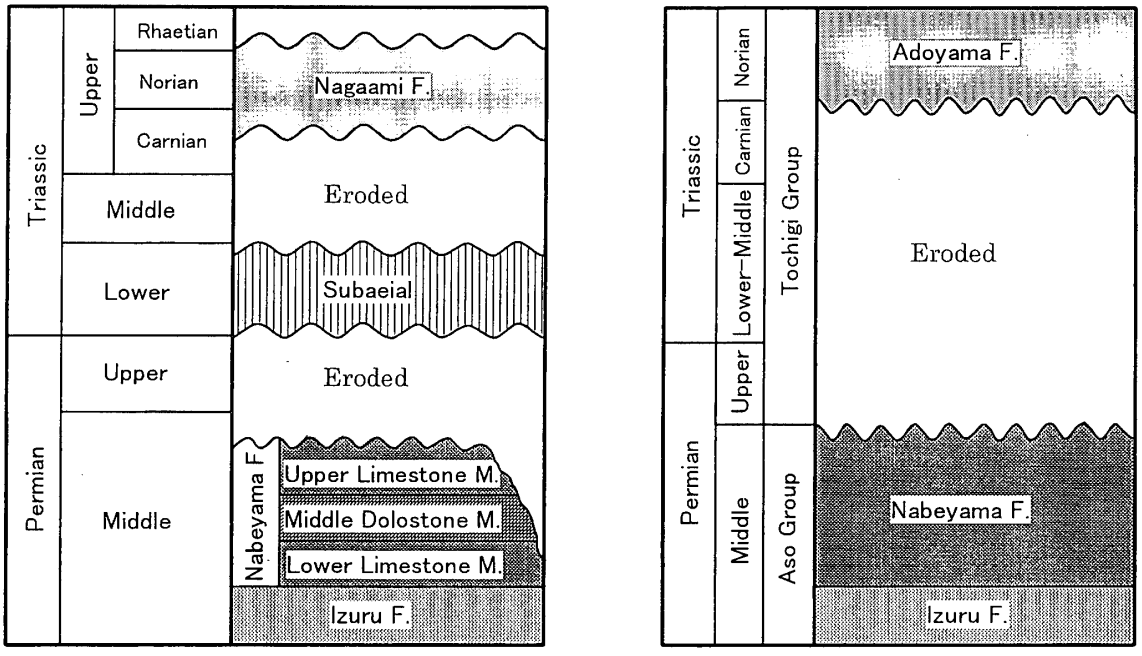

Matsuda and Iijima (1989)

Igo and Igo (1977), Kobayashi (1979)

Fig. 1-b. Stratigraphic section of Kuzuu area. These two charts are quoted from Matsuda and Iijima (1989) and from Igo and Igo (1977) and Kobayashi (1979), respectively.

cherts and shales in Igo and Igo (1977) and Kobayashi (1979).

Thus the Nabeyama Formation started as a carbonate sequence on a basaltic seamount of the Middle Permian Izuru Formation, and the deposition of biogenic carbonates continued by the end of Permian. And then, the carbonate succession was subjected to erosion in the Early to Middle Triassic. The Upper Permian carbonate sequence was eroded away and only the Middle Permian one has survived as noted above. The Kuzuu limestone-dolostone complex associated with coeval mafic volcanics corresponds to coral-reef limestones and shallow carbonate sequences on the summit of basaltic seamounts in the present-day western Pacific. This type of limestone-basaltic rock associations of the Late Paleozoic formed in open-sea realm are frequently found as exotic accretionary terranes in Japanese Islands (Sano and Kanmera, 1988).

SAMPLES AND ANALYTICAL METHODS

(1) Samples

The carbonate rocks of Nabeyama Formation were sampled in the Yoshizawa Mine in Kuzuu. Three samples (TKC-1~3) are from Lower Limestone, four samples (TKC-4~7) from Middle Dolostone, and four samples (TKC-8~11) from Upper Limestone. A reference carbonate rock (JDo-1) issued from Geological Survey of Japan is prepared from Middle Dolostone in the Yoshizawa Mine (Ando et al., 1990). Hence we have analyzed JDo-1 as an additional sample of this study. All REEs including Y, major and minor elements, and $^{87}Sr/^{86}Sr$ isotopic ratio have been determined for the twelve samples. In order to determine Sr isotopic ratios of calcite and dolomite in each dolostone sample, it was leached with acetic acid. Leachate and residue correspond to calcite and dolomite fractions of each dolostone sample, respectively.

(2) Chemical analysis of REEs and major and minor elements

The samples of Kuzuu carbonate rocks scarcely contain non-carbonate impurities as noted before. HCl-soluble parts of respective samples were analyzed for all REEs including Y, Ca, Mg, Ba, Sr, Na, Al, Fe, Mn and P by ICP-AES.

REE and Y were separated from matrix elements by the method of coprecipitation with Fe hydroxide and cation-exchange chromatography described elsewhere (Kawabe et al., 1991 and 1994). In brief, an aliquot of each powdered sample weighing about 10 g was dissolved by HCl. It was filtered to remove insoluble organic matter. Fe(III) of 20 mg was added to the filtrate, and its pH was adjusted to be 6.5 by ammonia water. REE and Y were precipitated with $Fe(OH)_3$ and then the precipitate was filtered. Again Fe(III) of 14 mg was added to the filtrate, and the coprecipitation was repeated in order to make the recoveries of REE and Y satisfactory. The first and second precipitates of $Fe(OH)_3$ were combined and dissolved by HCl again, and the coprecipitation procedure as before was repeated once more. This repetition is necessary to reduce coexistent Ca concentration. The final precipitates of $Fe(OH)_3$ were dissolved, and REE and Y in the solution were separated from matrix elements by a cation-exchange resin column (ø=1 cm × 11 cm) of Bio-Rad 50Wx8. REE and Y were determined by ICP-AES spectrometer of SEIKO SPS-1500R. An ultrasonic

nebulizer was used for the determinations of Pr, Tb, Ho, and Tm. The others were determined by using a conventional coaxial pneumatic nebulizer.

For determining Ba, Sr, Na, Al, Fe, Mn and P, another aliquot weighing 0.5 g was dissolved by HCl. The filtrate was used for their determinations by ICP-AES. In order to eliminate matrix effect of coexisting Ca, the same quantity of Ca was added to standard solutions. An aliquot of this sample solution was diluted in 100 times, and then it was used for ICP-AES determinations of Ca and Mg.

(3) $^{87}Sr/^{86}Sr$ isotopic ratio

For determining $^{87}Sr/^{86}Sr$ isotopic ratio of each bulk sample, another aliquot weighing 0.25 g was dissolved in HCl, and the dissolved Sr was purified by a cation-exchange resin column (ø=1 cm × 11 cm) of Bio-Rad 50Wx8. In order to determine $^{87}Sr/^{86}Sr$ isotopic ratios of dolomite and calcite in the samples having high contents of dolomite (TKC-4~9 and JDo-1), aliquots of the powdered samples 1.0 g were leached with 0.1 M acetic acid for 12 hours at the room temperature. The residues were dissolved in HCl. We regard the Sr in leachate and residue as the Sr contained in calcite and dolomite, respectively. They were purified by the cation-exchange column as above.

Sr isotopic compositions of all the bulk samples and calcite-dolomite pairs in seven samples were determined by the thermal ionization mass spectrometer of VG Sector 54-30 according the method by Asahara et al. (1999). The $^{87}Sr/^{86}Sr$ isotopic ratio of NIST-SRM 987 determined during the runs for analyzing the samples of this study was 0.710247±7 (2σ, n=19). All the $^{87}Sr/^{86}Sr$ isotopic ratios of our samples have been corrected by normalizing the $^{87}Sr/^{86}Sr$ isotopic ratio of NIST-SRM 987 to 0.71024.

RESULTS AND DISCUSSION

(1) Chondrite-normalized REE patterns with seawater-like tetrad effects

Analytical results of REE and Y for the Kuzuu carbonate rocks are listed in Table 1, and those of major and minor elements are in Table 2. Ce and Eu anomalies in this paper are defined as below,

$$\log(Ce/Ce^*)\equiv\log\{Ce_n/(La_n^2 \times Nd_n)^{1/3}\} \text{ and } \log(Eu/Eu^*)\equiv\log\{Eu_n/(Sm_n \times Gd_n)^{1/2}\}, \quad (1)$$

where subscript "n" indicates the normalized value by CI chondrite (Anders and Grevesse, 1989). When analytical data of REE include Pr analyses as our data of Table 1, the Ce anomaly is to be calculated by $\log\{Ce_n/(La_n \times Pr_n)^{1/2}\}$. We will compare the Ce anomalies of our carbonate samples with those of modern seawater samples. Majority of reliable REE data for modern seawater samples are those by the isotope-dilution thermal ionization mass-spectrometry, and the seawater Ce anomalies are calculated by (1) using polyisotopic REE of La and Nd. In order to compare the Ce anomalies of our carbonate samples with those of seawater samples, we also calculate the Ce anomaly without using the Pr analysis.

The REE and Y analyses of JDo-1 have already been reported in Kawabe et al. (1998). The REE and Y abundances in Kuzuu samples are normalized by CI chondrite and shown in Figs. 2-a, b and c. The chondrite-normalized REE and Y patterns exhibit the following common characteristics: (i) light REE enrichments with concave

Table 1. Analytical results of REEs in Kuzuu carbonate rocks[*1]

	Lower Limestones			Middle Dolostones					Upper Limestones				Pacific Seawater
	TKC-1	TKC-2	TKC-3	TKC-4	TKC-5	TKC-6	TKC-7	JDo-1[*3]	TKC-8	TKC-9	TKC-10	TKC-11	(depth = 381 m)[*4]
REE (ppm)													REE (ppt)
La	9.52	5.05	5.08	11.2	5.93	4.85	5.80	7.91	12.3	5.95	8.96	4.68	1.403
Ce	5.07	1.93	1.93	4.80	1.62	1.04	1.20	2.16	3.93	1.22	1.93	1.35	0.478
Pr	1.27	0.58	0.61	1.48	0.75	0.57	0.65	0.99	1.72	0.61	1.19	0.59	0.231
Nd	5.22	2.49	2.64	6.24	3.22	2.46	2.77	4.25	7.20	2.57	5.12	2.53	1.141
Sm	0.826	0.395	0.430	1.01	0.500	0.385	0.414	0.706	1.19	0.401	0.795	0.388	0.248
Eu	0.211	0.098	0.106	0.237	0.117	0.091	0.095	0.16	0.285	0.099	0.185	0.094	0.071
Gd	0.962	0.514	0.578	1.23	0.648	0.531	0.545	0.91	1.52	0.564	1.06	0.514	0.414
Tb	0.133	0.074	0.082	0.165	0.082	0.079	0.073	0.128	0.214	0.078	0.147	0.073	0.067
Dy	0.798	0.481	0.526	1.04	0.537	0.483	0.468	0.774	1.32	0.502	0.925	0.466	0.523
Ho	0.165	0.108	0.117	0.215	0.116	0.112	0.104	0.176	0.292	0.113	0.206	0.103	0.146
Er	0.442	0.288	0.336	0.609	0.335	0.339	0.311	0.469	0.853	0.322	0.586	0.302	0.470
Tm	0.052	0.040	0.043	0.070	0.041	0.041	0.037	0.056	0.096	0.037	0.073	0.035	0.063
Yb	0.312	0.231	0.229	0.380	0.215	0.235	0.206	0.31	0.556	0.199	0.379	0.196	0.393
Lu	0.044	0.033	0.031	0.051	0.030	0.033	0.029	0.044	0.076	0.028	0.054	0.028	0.065
Y	9.11	7.03	7.36	13.2	7.56	7.63	7.62	10.2	17.4	7.78	12.5	6.92	7.89
Y/Ho (molar ratio)	103	120	117	114	121	126	136	108	110	128	112	124	(=100)
La/Yb (molar ratio)	38.0	27.2	27.6	36.8	34.3	25.7	35.1	31.8	27.6	37.3	29.4	29.7	4.5
Ce anomaly[*2]	-0.50	-0.63	-0.64	-0.60	-0.79	-0.89	-0.89	-0.79	-0.73	-0.88	-0.90	-0.76	-0.75
Eu anomaly[*2]	-0.14	-0.18	-0.19	-0.19	-0.20	-0.22	-0.22	-0.22	-0.19	-0.20	-0.21	-0.19	-0.17

[*1] All the values are for HCl-soluble portions of the respective samples.

[*2] Ce and Eu anomalies are calculated by $\log[Ce_n/(La_n^2 \times Nd_n)^{1/3}]$ and $\log[Eu_n/(Sm_n \times Gd_n)^{1/2}]$ respectively. The subscript n indicates the nomalized abundance by CI chondrite.

[*3] GSJ reference carbonate rock. The results are cited from Kawabe et al. (1998).

[*4] REE concentrations in the Pacific seawater at depth of 381 m (Piepgras and Jacobsen, 1992) and the estimates for monoisotopic REE concentrations by the method of Kawabe et al. (1998): It is also assumed that the molar Y/Ho ratio=100 according to Zhang et al. (1995).

Table 2. Analytical results of major and minor elements in Kuzuu carbonate rocks[*1]

	Lower limestones			Middle dolostones					Upper limestones			
	TKC-1	TKC-2	TKC-3	TKC-4	TKC-5	TKC-6	TKC-7	JDo-1[*2]	TKC-8	TKC-9	TKC-10	TKC-11
Ca(%)	35.4	37.8	36.8	25.2	20.4	23.8	26.4	24.2	35.9	31.6	37.1	38.6
Mg(%)	1.20	0.363	0.268	9.87	9.40	11.1	9.13	10.8	1.87	5.73	0.263	0.226
Fe(ppm)	661	404	534	1282	86.1	46.0	117	135	397	50.3	33.9	36.8
Mn(ppm)	25.4	24.1	14.7	25.5	17.5	23.4	15.9	47.4	14.7	7.86	15.6	14.4
P(ppm)	83.4	96.7	69.8	120	188	121	587	151	125	99.2	167	56.3
Al(ppm)	185	99.2	44.9	87.5	41.7	31.1	48.1	40.9	312	22.2	23.1	7.61
Sr(ppm)	234	222	163	112	136	114	99.1	116	103	129	150	194
Ba(ppm)	4.08	3.19	11.1	3.28	5.84	2.54	3.16	5.83	4.24	3.69	4.83	8.27
Na(ppm)	31.4	29.6	34.4	43.5	57.9	53.3	69.0	81.8	49.1	37.0	22.0	16.6
Mg/Ca (molar ratio)	0.056	0.016	0.012	0.646	0.760	0.771	0.570	0.735	0.086	0.299	0.012	0.010

[*1] All the data are for HCl-soluble portions of the respective samples.
[*2] GSJ reference carbonate rock. Analytical results in this study are listed.

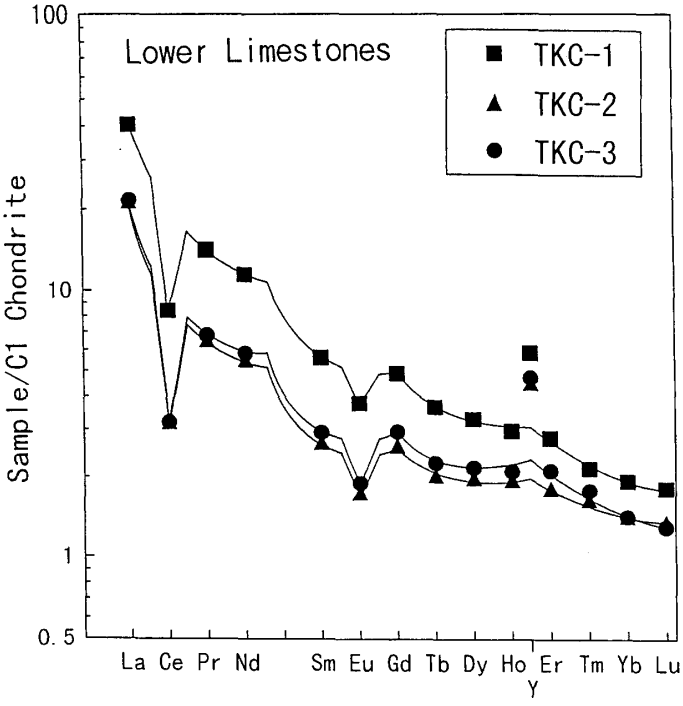

Fig. 2-a. Chondrite-normalized REE and Y abundance patterns for Kuzuu Lower Limestomes. REE and Y data for CI chondrite (Anders and Grevesse, 1989) are used for normalization.

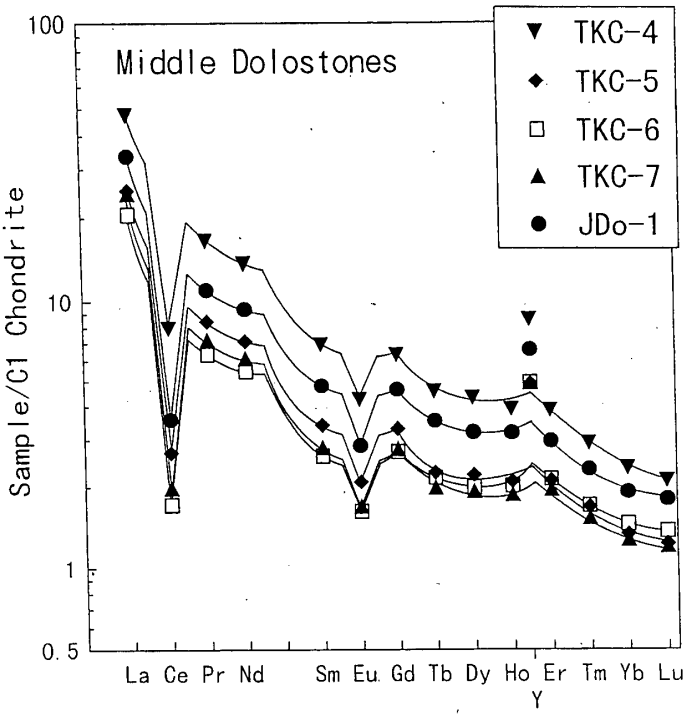

Fig. 2-b. Chondrite-normalized REE and Y abundance patterns for Kuzuu Middle Dolostones. REE and Y data for CI chondrite (Anders and Grevesse, 1989) are used for normalization.

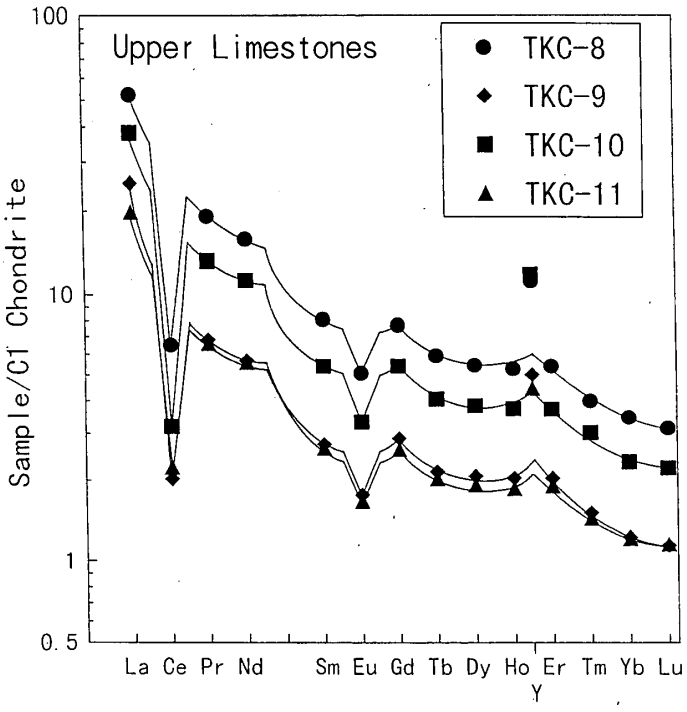

Fig. 2-c. Chondrite-normalized REE and Y abundance patterns for Kuzuu Upper Limestomes. REE and Y data for CI chondrite (Anders and Grevesse, 1989) are used for normalization.

tetrad effect variations, (ii) quite large negative Ce anomalies, (iii) small negative Eu anomalies, and (iv) high Y/Ho ratios much grater than the chondritic Y/Ho one. These REE and Y features are also observed in chondrite-normalized REE and Y patterns for seawater (Kawabe et al., 1991 and 1998). Kuzuu carbonate rocks have quite high Y/Ho ratios, i.e., all their molar Y/Ho ratios are equal to 100 or more. This can be seen in the chondrite-normalized REE and Y patterns for Kuzuu samples as "positive Y anomalies". Terrigenous materials like shales have Y/Ho ratios similar to the chondritic one. Therefore the "positive Y anomalies" as well as the large negative Ce anomalies cannot be explained, if the carbonate rocks contain significant amounts of terrigenous materials. This is compatible with the geological inference that they were formed on a basaltic seamount in open-sea realm without effect of terrigenous material inputs.

The REE and Y abundance patterns for the carbonate rocks normalized by present-day Pacific seawater are shown in Figs. 3-a, b and c. The REE data for a Pacific water sample at a depth of 381 m (Piepgras and Jacobsen, 1992) are used for normalization. The monoisotopic REE (Pr, Tb, Ho and Tm) abundances in the Pacific water are estimated by the method of Kawabe et al. (1998). The yttrium abundance is also estimated by assuming that the molar Y/Ho ratio of Pacific water is 100 as is reported by Zhang et al. (1994). The seawater REE data are listed in Table 1. Note that the seawater REE data for the Pacific water at a depth of 381 m is used for normalization. This water depth is greater than the maximum water depth transparent to sunlight (~200 m), which is related to the later our discussion on the basis of Ce

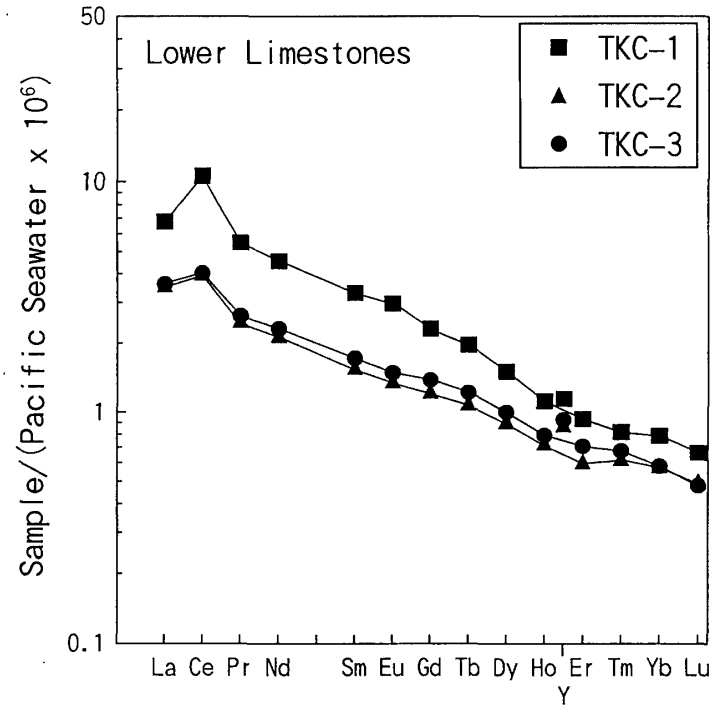

Fig. 3-a. Seawater-normalized REE and Y abundance patterns for Kuzuu Lower Limestomes. The REE data for a Pacific water sample at a depth of 381 m (Piepgras and Jacobsen, 1992) listed in Table 1 are used for normalization.

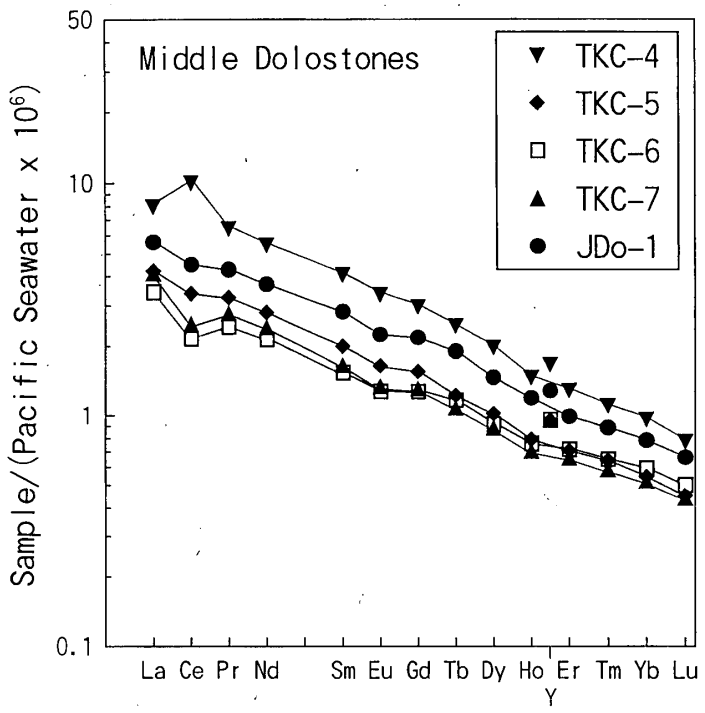

Fig. 3-b. Seawater-normalized REE and Y abundance patterns for Kuzuu Middle Dolostones. The seawater REE data for normalization are the same as in Fig. 3-a.

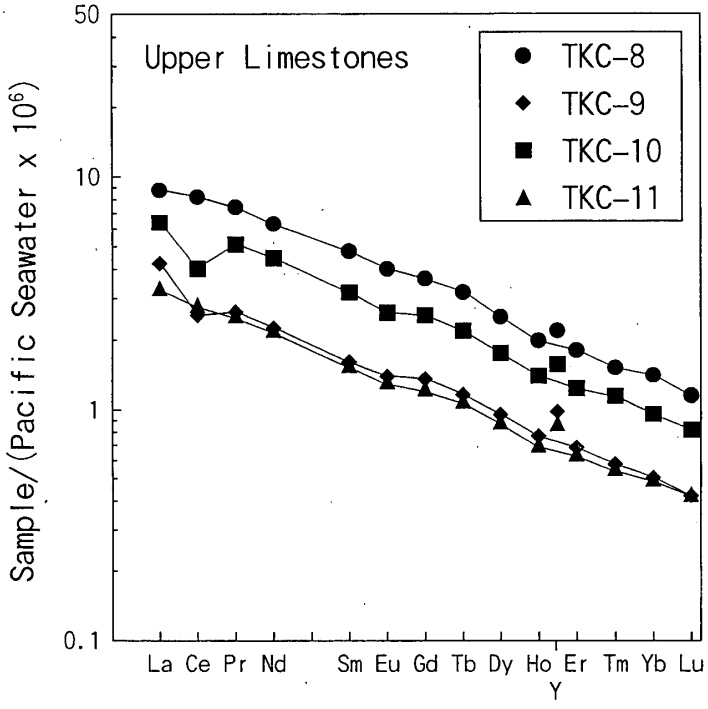

Fig. 3-c. Seawater-normalized REE and Y abundance patterns for Kuzuu Upper Limestones. The seawater REE data for normalization are the same as in Fig. 3-a.

anomalies of Kuzuu samples.

In the seawater-normalized REE and Y patterns for the Kuzuu carbonate rocks, there can be seen approximately linear trends of light REE enrichment without obvious tetrad effects and Eu anomalies. Ce anomalies and Y fractionation from Ho are also less conspicuous in the seawater-normalized patterns than those in the chondrite-normalized ones. Hence the concave tetrad curves seen in chondrite-normalized REE patterns for the Kuzuu carbonate rocks (Figs. 2-a, b and c) are clearly indicating the signature of seawater tetrad effect.

(2) High enrichments of REE and Y in Kuzuu carbonate rocks

The seawater-normalized REE patterns for all the Kuzuu samples are fairly parallel to one another, although there still remain small Ce anomalies which are slightly different within each carbonate rock member. In order to see possible differences in the REE and Y pattern between the Middle Dolostone and the other limestone members, we have calculated average REE and Y abundance patterns for the three members. Figure 4 shows the average abundance patterns normalized by the same Pacific water REE used in Figs. 3-a, b and c, together with the range of their REE enrichments. In Fig. 4, the REE distribution coefficients normalized by Ca,

$$K_d=(REE/Ca)_{carbonate}/(REE/Ca)_{sw\ solution}, \quad (2)$$

between the pairs of modern coral/seawater (Sholkovitz and Shen, 1995) and of Holocene microbialite/seawater (Webb and Kamber, 2000) are plotted, along with the experimental results of K_d for calcite-overgrowth/synthetic seawarer (Zhong and Mucci, 1995). The values of Limestone/(Seawater $\times$ 10^6), which are shown in Figs. 3 and 4 as the seawater-normalized REE patterns, can be converted to K_d values by using the molar Ca concentration of 10^{-2} M in seawater:

$$K_d= 10^3 \times \{Limestone/(Seawater \times 10^6)\}. \quad (3)$$

The two vertical scales of Fig. 4 correspond to (3). Hence K_d values evaluated from REE data for the Kuzuu Lower and Upper Limestones and the Pacific water are in the range from 10^2 to 10^4.

In the case of our dolostone samples from the Middle Dolostone member, the conversion by (3) is not immediately made, because they are composed of dolomite and subordinate amounts of calcite. Small weight changes associate with the substitutions of Ca in calcite by Mg. The change in weight is only 8%, even when all the calcite changes to dolomite. Therefore it is actually insignificant when we discuss about REE distribution coefficients in the logarithmic scale. The average REE abundances in the samples from the Middle Dolostone are actually the same as those in the Lower and Upper Limestones, except for small differences in Ce abundances (Fig. 4). This may be a line of evidence suggesting that precursors of the dolostones were the limestones which already incorporated the seawater REE and Y like the limestones in the Lower and Upper Limestone members. It is also suggested that the seawater REE and Y signatures were not altered by the later dolomitization. Therefore, molar (Mg + Ca) contents of dolostone samples are read as the Ca contents of the limestone precursors, and the conversion by eq. (3) is applicable to the dolostone samples. Miura and

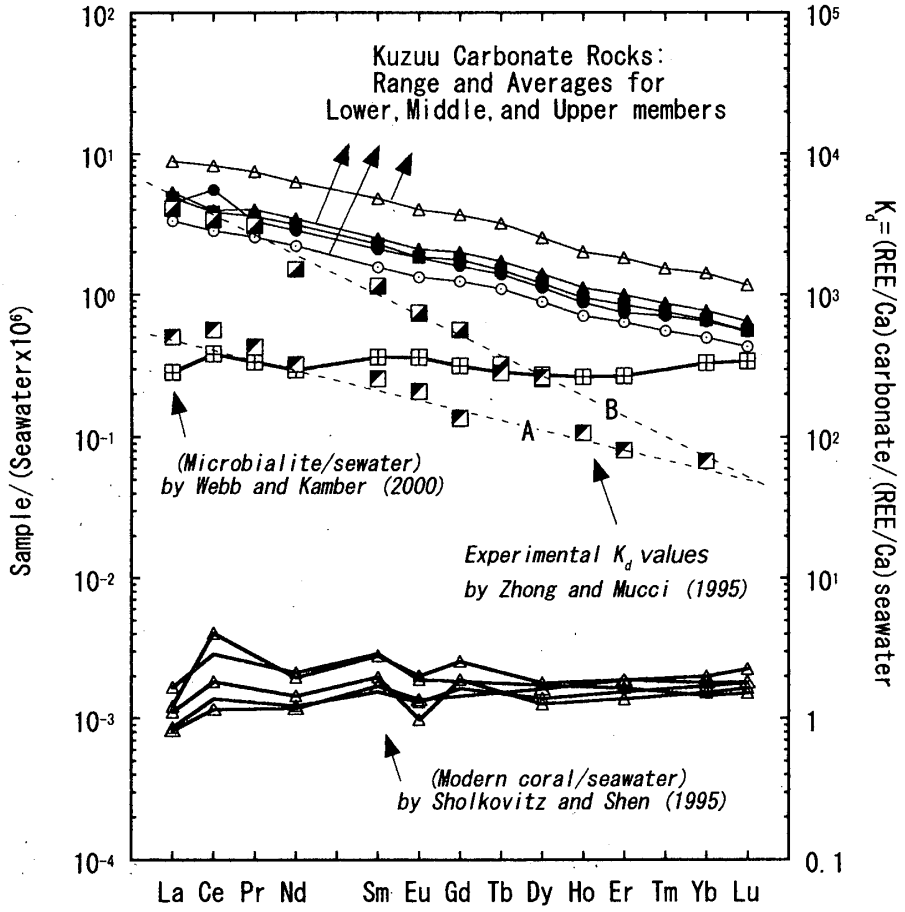

Fig. 4. Averaged REE abundance ptterns of Lower Limestone (filled circles), Middle Dolostone (filled squares), and Upper Limestone (filled triangles) of Kuzuu carbonate rocks normalized by the Pacific seawater in Figs. 3-a, b, and c. TKC-8 (small open triangles) and TKC-11 (small open circles) correspond to the upper and lower limits of REE enrichments in the Kuzuu samples, respectively. The distribution coefficients K_d given by (REE/Ca) abundances ratios between modern corals and coexisting seawater in Bermuda (Sholkovitz and Shen, 1995) and those for the pair of average Holocene microbialite and seawater (Webb and Kamber, 2000) are shown for comparison. The two sets of experimental K_d values by Zhong and Mucci (1995) are also plotted (half-filled squares with dashed lines of A and B). The set of smaller K_d values (A) is for experimental seawater solutions with REE (La-Eu) concentrations of 10 nM and the other REE ones of >10 nM. Another set of larger K_d values (B) is for the solutions with REE (La-Dy) concentrations of 70 nM and the other REE ones of >70 nM. The relationship between two vertical scales is explained in the text.

Kawabe (2000) demonstrated that the limestone sample from Kuzuu Upper limestone member (TKC-10) is dolomitized in reaction with 2 M $MgCl_2$ solution at 150°C for 10–20 days. About 90% of calcite was transformed into dolomite, but REE and Y abundance charactristics of the original limestone sample (Fig. 2-c) was preserved in the dolomitized product, supporting our interpretation of the field data.

Sholkovitz and Shen (1995) reported REE concentrations in modern corals and coexistent seawater. The REE/Ca ratios of modern corals are approximately one-thousandth of REE/Ca ratios of Kuzuu carbonate rocks (Fig. 4). The La/Yb ratios of

the corals are about one-tenth of those ratios of the Kuzuu samples, and K_d values evaluated from the pair of modern coral and seawater are approximately unity. Thus the seawater REEs incorporated into the modern biogenic carbonates can never explain the high (REE/Ca) ratios observed in the Kuzuu carbonate rocks, because they are 10^2 to 10^4 times as high as the seawater (REE/Ca) ratios. We interpret that seawater REE and Y were incorporated into the carbonate rocks, when their original biogenic carbonates re-crystallized to inorganic calcite. Our interpretation is supported by the experimental REE partitioning between calcite-overgrowths and seawater solutions (Zhong and Mucci, 1995) cited in Fig. 4. The precursor limestones of the Middle Dolostone member were subjected to dolomitization subsequently, but the seawater REE and Y signatures of the limestone precursors have been preserved in the resultant dolostones as shown by the experimental result of Miura and Kawabe (2000).

Webb and Kamber (2000) reported REE abundances in Holocene microbialites. The K_d values for the Holocene microbialite/seawater pair are approximately 300 across the entire REE series, but they indicate no trend of light REE enrichment relative to seawater (Fig. 4). Therefore, REE enrichemnt features of Kuzuu carbonate rocks cannot be explained by K_d from Holocene microbialites at all. The seawater-normalized REE patterns for all the Kuzuu samples show light REE enrichment trends commonly, and similar results of the REE analyses for the Late Paleozoic seamount-type limestones in central Japan have been reported by Tanaka et al. (2003). The $\log K_d$ values from the Kuzuu samples are comparable with the experimental results of REE enrichments into calcite-overgrowths from REE-doped seawater solutions (Zhong and Mucci, 1995) in view of the magnitude of K_d and the light REE enrichment trend. The K_d values inferred from the pairs of Holocene microbialite/seawater or modern coral/seawater cannot account for the REE features of the Kuzuu samples.

The reported experimental REE distribution coefficients of K_d by Zhong and Mucci (1995) are ranging from 10^2 to 10^4, but the variation patterns of $\log K_d$ are depending on REE concentrations in experimental seawater solutions (Fig. 4). The K_d values (A) for solutions with lower REE concentrations (10 nM) for light REE show almost the same trend of light REE enrichment as those in the Kuzuu samples, whereas the K_d values are one order of magnitude smaller. On the other hand, the K_d values (B) for solutions with higher REE concentrations (70 nM) for light REE are roughly comparable with those from the Kuzuu samples, but the light REE enrichment trend is more obvious than those observed in the Kuzuu carbonate rocks (Fig. 4). The laboratory results by Zhong and Mucci (1995) are not perfectly compatible with the field data of the Kuzuu carbonate rocks. This situation is the same as in another field data set from the Late Paleozoic seamount-type limestone in central Japan (Tanaka et al. 2003), suggesting the importance of further experimental studies of K_d for the pair of calcite and seawater solution.

Recently Tanaka et al. (2004) reported the new experimental results of REE partitioning between calcite and aqueous solution at 25°C, and proposed a method to infer REE abundance patterns for the ancient seawater associated with the diagenetic process of marine biogenic carbonates. Tanaka et al. (2004) successfully estimated REE abundance patterns of the late Paleozoic seawater by this method using the REE analyses of Ishimaki and Tahara limestones in central Japan (Tanaka et al., 2003). The

REE patterns for the late Paleozoic seawater obviously resemble those for moderately deep water in the modern ocean. The method utilizes only the experimental REE partition coefficients and the REE analyses of ancient marine limestone samples. This method is superior to the use of seawater-normalized REE patterns like Figs. 3-a, b, and c, in which the REE data for present-day ocean water are used and the ancient seawater is implicitly assumed to resemble the present-day seawater. Whether the ancient seawater associated with Kuzuu or other marine carbonate rock suite had the same REE characteristics as the modern seawater is to be demonstrated without assuming such resemblance implicitly. The application of the method by Tanaka et al. (2004) to Kuzuu samples will be presented elsewhere (Tanaka and Kawabe, in preparation).

(3) Ce anomalies of carbonate rocks and water depth of diagenetic seawater

The chondrite-normalized REE patterns for all the Kuzuu carbonate rocks do not show the same negative Ce anomalies (Figs. 2-a, b and c). In particular, the magnitudes of negative Ce anomalies of the three samples from the Lower Limestones (TKC-1~3) and one sample from the lowest part of the Middle Dolostone (TKC-4) are smaller than those of the other samples. The four carbonate rocks from the bottom part of Kuzuu succession can be distinguished from the others in the plot of Ce anomaly vs. Fe content and in the plot of Ce anomaly vs. Y/Ho ratio (Figs. 5-a and b). The four samples with smaller negative Ce anomalies have higher Fe contents, and the sample with the smallest negative Ce anomaly shows the lowest Y/Ho ratio. This may suggest some influence by Fe(III) oxyhydroxide colloids. Experimental REE and Y partition coefficients between Fe(III) oxyhydroxide precipitates and seawater-like solution indicate positive Ce anomaly and negative Y anomaly (Kawabe et al., 1999). Ferromanganese crusts in the Pacific also show positive Ce anomalies and the Y/Ho ratios less than the seawater Y/Ho ratio (Bau et al., 1996; Ohta et al., 1999). As described above, the carbonate rock succession of Nabeyama Formation conformably overlies the Izuru Formation comprising mainly submarine mafic pyroclastic rocks and lavas. Therefore it is likely that fluids interacted with submarine volcanic materials may have polluted the bottom part of overlying carbonate succession with Fe(III) oxyhydroxide colloids. But such fluids did not influenced the upper part of the succession. The average Ce anomaly, $\log(Ce/Ce^*)$, and its one-sigma range for the four samples from the bottom part is $-(0.59\pm0.06)$, whereas those for the other samples is $-(0.83\pm0.07)$. The negative maximum of Ce anomaly of seawater incorporated into the Kuzuu carbonate rocks must be −0.9.

In order to gain further insight into the Ce anomalies of Kuzuu carbonate rocks, it is important to refer to the vertical distribution of Ce anomaly of present-day ocean waters (Fig. 6). Depth profiles of seawater Ce anomalies in water columns in Pacific, Atlantic, and Indian Oceans (German and Elderfield, 1990; Piepgras and Jacobsen, 1992; Bertram and Elderfield, 1993; Sholkovitz et al., 1994; German et al., 1995) are cited in Fig. 6. Although the profiles are not exactly the same among the water columns, there is a definite general trend as follows: the Ce anomaly of surface water shallower than 200 m is within the range of $-(0.4\pm0.2)$, and the anomaly rapidly becomes more negative with increasing water depth until 1,000 m, and then

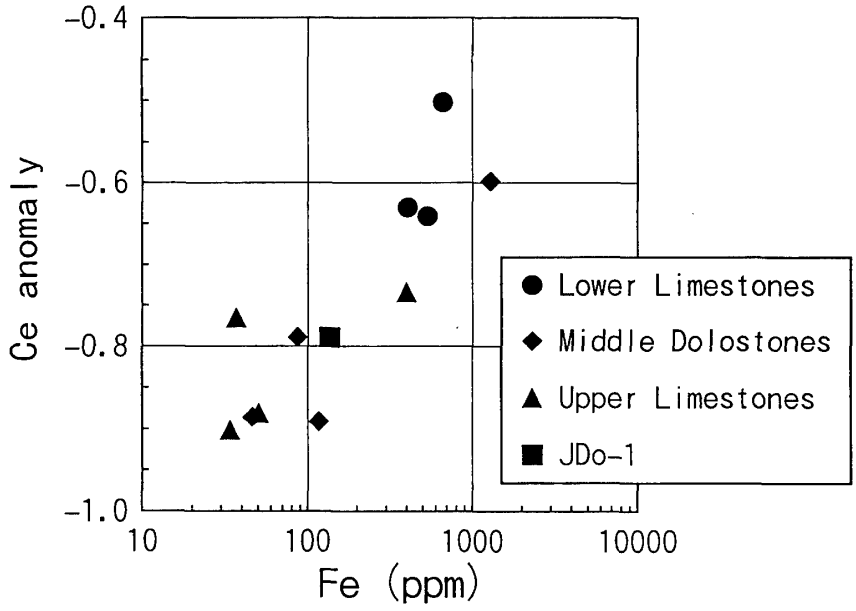

Fig. 5-a. Plot of Fe content vs. Ce anomaly of Kuzuu carbonate rocks.

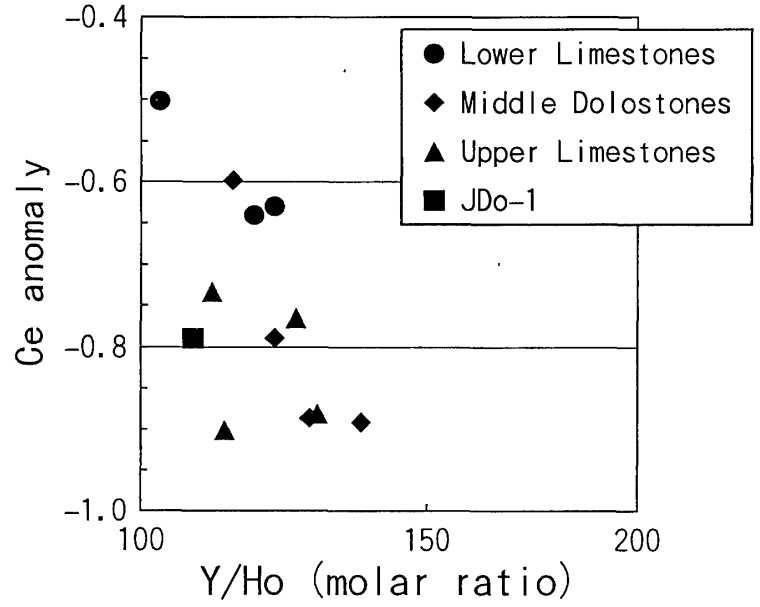

Fig. 5-b. Plot of Y/Ho molar ratio vs. Ce anomaly of Kuzuu carbonate rocks.

it takes an approximately constant value of 1 –(1.1±0.1) at depths greater than 1,000 m. The reason for this characteristic depth profile of seawater Ce anomaly can be understood from elementary processes controlling Ce redox chemistry in ocean water; (i) oxidative scavenging of Ce(III) as particulate Ce(IV) from seawater solution in ocean water column, (ii) photoinhibitation of Ce(III) oxidation in surface water, and (iii) circulation of oxygenated cold water being produced in polar regions across different ocean basins (Byrne and Sholkovitz 1996). Possibly the elementary processes

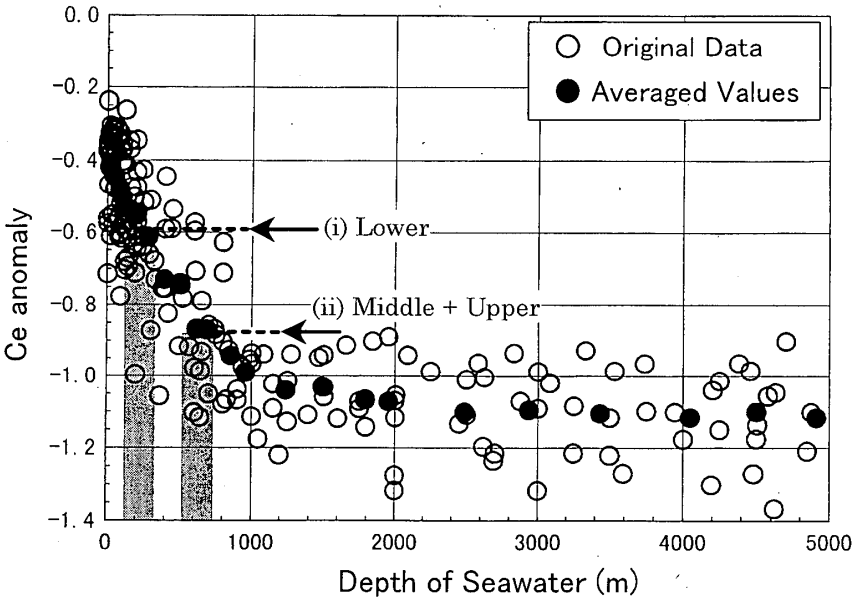

Fig. 6. Plot of Ce anomaly vs. water depth for modern seawater samples. Original data (opencircles) are from German and Elderfield (1990), Piepgras and Jacobsen (1992), Bertram and Elderfield (1993), Sholkovitz et al. (1994), German et al. (1995) and Zhang and Nozaki (1996). Filled circles are moving averages of Ce anomalies with respect to water depth by us. Ce anomalies for the samples from Kuzuu Middle and Upper members (TKC-5~11 and JDo-1) are (–0.76 ~ –0.90). The maximum value of –0.9 is indicated by an arrow. Another arrow indicates the average Ce anomaly (–0.59±0.06) for the four samples (TKC-1~4) from the part succession including the Lower member samples.

have been operative throughout the Phanerozoic time, since the three processes are driven by physico-chemical principles rather than the geological settings. Hence it seems conceivable that such a depth profile of log(Ce/Ce*) was present in the past ocean water (Tanaka et al., 2003).

In Fig. 6, we have shown the average Ce anomaly (–0.59±0.06) for the four samples from the bottom part and the negative maximum Ce anomaly (–0.9) in the other samples from upper parts of Kuzuu carbonate rock succession. The average Ce anomaly in the latter is –(0.83±0.07). If we assume that the vertical profile of the Ce anomaly of the present-day ocean water is comparable with that of Middle Permian ocean water, the Ce anomalies of (–0.76 ~ –0.9) in the Upper Limestone and majority of the Middle Dolostone suggests that Ce and the other REE and Y were incorporated into the carbonate rocks from the seawater at depths of 600–800 m. The range of water depth between 600 and 800 m is understood in such a way that the diagenetic re-crystallization of biogenic carbonates to calcite occurred under the condition of sufficient supply of moderately deep seawater shallower than 1,000 m but deeper than several hundred meters. This water depth is too deep to develop accumulation of biogenic carbonates, suggesting that the limestone-capped basaltic seamount was submerged at least to the water depth as discussed in Tanaka et al. (2003).

(4) Sr isotopic ratios of Kuzuu carbonate rocks and Sr isotopic stratigraphy

The analytical results of $^{87}Sr/^{86}Sr$ ratios for Kuzuu carbonate rocks are summarized

in Table 3. The Sr isotopic ratios for all the bulk samples are between 0.7073 and 0.7076. The range is compared with the data points for Late Paleozoic seawater $^{87}Sr/^{86}Sr$ curve by Denison et al. (1994) in Fig. 7. All the data by Denison et al. (1994)

Table 3. Analitical results of $^{87}Sr/^{86}Sr$ isotope ratios in Kuzuu carbonate rocks*.

Samples		Bulk	Calcite	Dolomite	Difference (Cal. - Dol.)
Lower Limestones	TKC-1	0.707360			
	TKC-2	0.707283			
	TKC-3	0.707466			
Middle Dolostones	TKC-4	0.707591	0.707595	0.707471	0.000124
	TKC-5	0.707613	0.707626	0.707571	0.000054
	TKC-6	0.707284	0.707312	0.707208	0.000104
	TKC-7	0.707353	0.707353	0.707351	0.000001
	JDo-1	0.707513	0.707537	0.707369	0.000168
Upper Limestones	TKC-8	0.707421	0.707452	0.707178	0.000274
	TKC-9	0.707328	0.707339	0.707182	0.000157
	TKC-10	0.707421			
	TKC-11	0.707468			

* The two-sigma standard deviation for $^{87}Sr/^{86}Sr$ ratio of NIST-SRM987 was 0.000007(n=19) as noted in the text. Hence the differences in the isotopic ratio between calcite and dolomite are significant except for TKC-7.

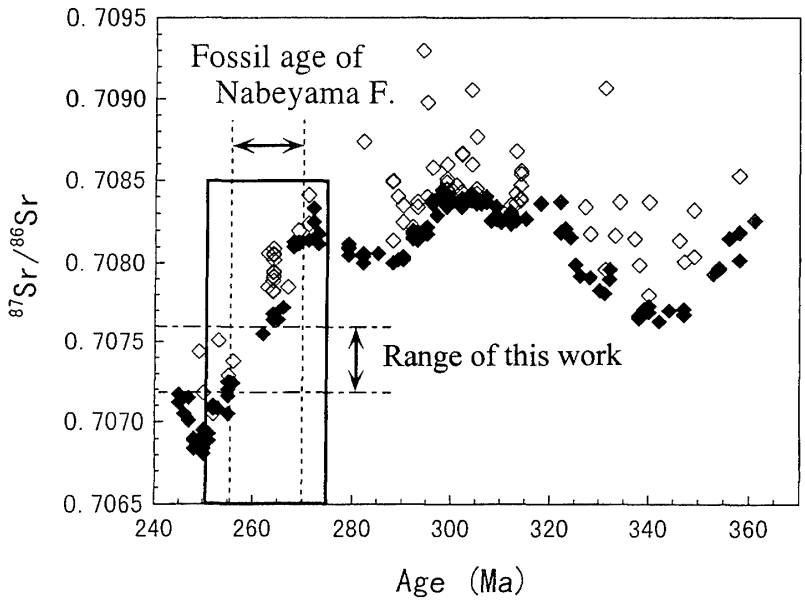

Fig. 7. The Late Paleozoic seawater $^{87}Sr/^{86}Sr$ curve by Denison et al. (1994). Filled diamonds are the data points which have retained the original seawater Sr isotopic ratios, and open diamonds are those altered apparently from the original seawater Sr isotope ratios or those with significant errors in the age assignment (Denison et al., 1994). The range of $^{87}Sr/^{86}Sr$ ratios for all the samples of Kuzuu carbonate rocks in this study is shown, along with the span of fossil age of Nabeyama Formation of Kuzuu carbonate rocks. An expanded plot of the boxed part is shown in Fig. 8.

are re-calculated by normalizing $^{87}Sr/^{86}Sr$ (NIST-SRM) to 0.71024 in the same way as in our analyses. We accepted the fusulinid fossil age of the Nabeyama Formation is 255–270 Ma (Harland et al., 1990; Ozawa, 1999 personal communication). This fossil age range is also indicated in Fig. 7. The seawater $^{87}Sr/^{86}Sr$ variation in Permian by Denison et al. (1994) and the fusulinid fossil age for the Nabeyama Formation give a range of $^{87}Sr/^{86}Sr$ ratio for the carbonate rocks between 0.7070 and 0.7082. This is in reasonable agreement with the observed range of $^{87}Sr/^{86}Sr$ ratios for all the bulk carbonate samples. It is concluded that the Kuzuu samples preserve the seawater $^{87}Sr/^{86}Sr$ ratio in the Middle Permian within the uncertainty of absolute age range of the fusulinid fossil zone.

The Late Paleozoic seawater $^{87}Sr/^{86}Sr$ curve by Denison et al. (1994) indicates a rapid decline from Early Permian to the end of Permian (Fig. 7). It is interesting to examine whether a systematic correlation between the $^{87}Sr/^{86}Sr$ ratio and stratigraphic order of the sample is recognized or not. In addition, it is also important to see whether there are systematic differences in the $^{87}Sr/^{86}Sr$ ratio between the respective pairs of calcite and dolomite. We have shown the boxed part of Fig. 7 in an expanded scale as Fig. 8. We have plotted all of our analyses including those for the pairs of

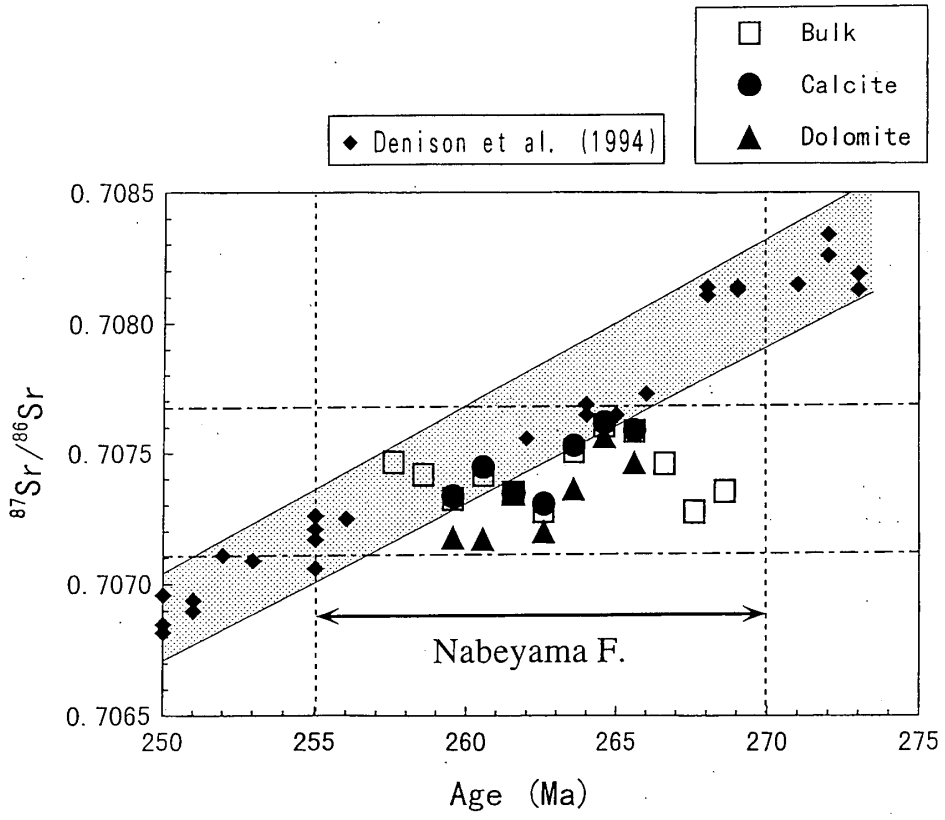

Fig. 8. The $^{87}Sr/^{86}Sr$ ratios for bulk, calcite and dolomite samples of Kuzuu carbonate rocks (Nabeyama Formation) compared with an extended plot of the seawater $^{87}Sr/^{86}Sr$ curve by Denison et al. (1994). The shaded area shows the variation trend of the seawater Sr isotopic ratio from 275 to 250 Ma. The data of $^{87}Sr/^{86}Sr$ ratios are plotted conventionally in the stratigraphic order with equal time intervals.

dolomite and calcite in Fig. 8. We only know the fusulinid age of the Nabeyama Formation as a range of 255–270 Ma, but we do not know the fossil ages of individual samples. Therefore we have plotted our data of $^{87}Sr/^{86}Sr$ ratios in the stratigraphic order conventionally with equal time intervals in the age range of Fig. 8.

Apparently there is no systematic correlation between the $^{87}Sr/^{86}Sr$ ratio and stratigraphic order of the sample. The average $^{87}Sr/^{86}Sr$ ratios and their one-sigma deviations for the bulk samples from the Lower Limestone, Middle Dolostone, and Upper Limestone members are 0.70737 (±10), 0.70747 (±15), and 0.70741 (±6), respectively. The Lower Limestone has a slightly lower average $^{87}Sr/^{86}Sr$ ratio than the other members. This is the reverse of what we expect from the reported temporal change of seawater $^{87}Sr/^{86}Sr$ ratio. In the discussion of Ce anomalies, however, we have pointed out that the bottom part of Kuzuu carbonate succession may have been polluted with Fe(III) oxyhydroxide colloids by fluids derived from underlying volcanic materials of the Izuru Formation. The slightly lower $^{87}Sr/^{86}Sr$ ratio of the Lower Limestone member might also be caused by the fluids, since basaltic rocks and related hydrothermal fluids have $^{87}Sr/^{86}Sr$ ratios much lower than the seawater ratio (Palmer and Edmond, 1989).

On the other hand, pairs of calcite and dolomite in the respective samples from the middle part of succession show small systematic differences in the $^{87}Sr/^{86}Sr$ ratio as listed in Table 3. In all the pairs, dolomite has always a lower $^{87}Sr/^{86}Sr$ ratio than coexisting calcite. The averaged difference in $^{87}Sr/^{86}Sr$ ratio is 1.3×10^{-4}. The rate of declining seawater $^{87}Sr/^{86}Sr$ ratio in Middle to Late Permian by Denison et al. (1994) shown in Fig. 8 is $(6\pm1) \times 10^{-5}$/Ma. Hence the systematic difference in the $^{87}Sr/^{86}Sr$ ratio between calcite and dolomite is calculated to be the time interval of about 2 Ma. This means that dolomitization followed the transformation of biogenic carbonate to calcite after a time interval of approximately 2 Ma. This time lag is not unreasonable when compared with dolomitization events in carbonate sequences of Niue Island (Aharon et al., 1987), Enewetak atoll (Ludwig et al., 1988) and Kita-daito-jima atoll (Ohde and Elderfield, 1992) in the Pacific.

(5) Kuzuu dolostone and models of dolomitization in late Cenozoic Pacific atolls

The Middle Permian Kuzuu limestone-dolostone complex was formed originally as a biogenic carbonate sequence on a basaltic seamount in open-sea realm. This interpretation primarily based on geological and paleontological data is further supported by the present REE and Sr isotopic study. Our geochemical data provide a constraint as to the diagenetic processes which the Kuzuu sequence experienced. It seems important to comment on the previously proposed models for dolomitization in late Cenozoic atoll sequences in the Pacific from the viewpoints we raised in this study.

Models for dolomitization in sedimentary carbonate columns on seamounts have been proposed for the sequences in Enewetak atoll (Saller and Koepinick, 1990), Niue Island (Schofield and Nelson, 1978; Rogers et al., 1982; Aharon et al., 1987), and Kita-daito-jima (Ohde and Elderfield, 1992). These are basically classified into the following three models: (i) calcite dissolution and dolomite precipitation by groundwater or meteoric water after upheaval of the carbonate sequence (Rogers et al., 1982), (ii)

dolomite precipitation in highly saline water in lagoon formed by evaporation of seawater (Schofield and Nelson, 1978; Ohde and Elderfield, 1992), and (iii) replacement of Ca-carbonate in reaction with moderately deep seawater convecting thermally inside of the carbonate succession (Aharon et al., 1987; Flood et al., 1996).

In the Kuzuu succession, there are no significant difference in REE and Y features between the Lower Limestone, Middle Dolostone and the Upper Limestone members, except for the point that carbonate rocks of a bottom part of succession tend to have smaller negative Ce anomalies than the other parts. The bottom part may have been polluted with Fe(III) oxyhydroxide colloids by fluids derived from underlying basaltic rocks of seamount. The carbonate rocks are highly enriched in REE and Y relative to modern biogenic carbonates or to seawater by factors of 10^2–10^4 when measured in molar REE/Ca and Y/Ca ratios. REE and Y were incorporated from the seawater at depths of 600–800 m, when biogenic carbonates re-crystallized to calcite. The dolomitization occurred in the middle part of the succession about 2 Ma later than the re-crystallization of biogenic carbonates to calcite, but the dolomitization did not alter the seawater REE and Y signatures of limestone precursors. In the case of carbonate successions on continental shelf of the Lower Carboniferous (Banner et al., 1988a) or of the Devonian (Qing and Mountjoy, 1994), dolomites preserving the REE features of limestone precursors have been reported.

If all the three dolomitization models as above allow to preserve the seawater REE and Y signatures of limestone precursors, and if the dolomitizing fluid has no relation with the fluid involved in the open-system re-crystallization of biogenic carbonates to calcite preceding the dolomitization, our results do not provide any constraint to evaluate the adequacy of the models. However, in the case of the Kuzuu succession, the open-system re-crystallization of biogenic carbonates to calcite occurred at water depths of 600–800 m, and then it was followed by the dolomitization only 2 Ma later. It may be unlikely that the dolomitizing fluid was totally different from the fluid involved in the open-system re-crystallization of biogenic carbonates to calcite. If we accept that the dolomitizing fluid is similar to that involved in the open-system re-crystallization of biogenic carbonates to calcite, the model (iii) is the most compatible with our results. The model (iii) emphasizes the importance of moderately deep seawater circulating in the carbonate sequence by thermal convection. Our suggestion that the bottom part of Kuzuu carbonate rocks were polluted with Fe(III) oxyhydroxide colloids, is also readily explained by the convective circulation of seawater.

CONCLUSIONS

(1) The carbonate rocks of the Middle Permian Kuzuu limestone-dolostone complex, central Japan, are highly enriched in REE and Y relative to modern biogenic carbonates or seawater by factors of 10^2–10^4 in molar REE/Ca and Y/Ca ratios. The $^{87}Sr/^{86}Sr$ ratios of bulk carbonate samples are ranging between 0.7073 and 0.7076, and their Sr isotopic stratigraphic age (260±5 Ma) coincides with their fusulinid fossil age (263±8 Ma).

(2) Chondrite-normalized REE patterns for the Kuzuu samples show large negative Ce anomalies, seawater-like tetrad effects and high Y/Ho ratios. The Ce anomalies of

the samples except those from a bottom part are comparable to those of present-day ocean waters at depths of 600–800 m. Their REE patterns normalized by the present-day Pacific seawater at a depth of 381 m, exhibit fairly smooth enrichment trends of light REE relative to heavy REE, which are similar to the reported experimental REE partitioning coefficients between calcite-overgrowths and seawater solutions. The K_d(REE/Ca:carbonate/seawater) values evaluated from the pairs of Holocene microbialite/seawater or modern coral/seawater cannot explain the REE features observed in the Kuzuu carbonate rocks. There is no significant difference in REE and Y features between the limestone and dolostone members.

(3) Biogenic carbonates deposited on a basaltic seamount in shallow water environment without influence of terrigenous material inputs. They were subsided to the water depths as suggested by their Ce anomalies. At the water depth, an open-system re-crystallization of the biogenic carbonates to calcite occurred, in which the seawater REEs and Y were incorporated into calcite. The carbonates of a bottom part of the succession have smaller negative Ce anomalies and higher Fe contents than the others, suggesting some pollution by the fluids with colloidal $Fe(OH)_3$ from underlying basaltic volcanics of the seamount.

(4) The Sr isotopic ratios of dolomite are slightly lower than those of coexistent calcite by 0.0002, which may be a time interval of about 2 Ma from the seawater $^{87}Sr/^{86}Sr$ curve for Middle to Late Permian. The dolomitization therefore occurred almost immediately after the re-crystallization of biogenic carbonate to calcite in relatively deep water, and did not alter the REE and Y features of limestone precursors. This is consistent with the recent diagenetic model for the carbonate sequences of Neogene atolls in the Pacific emphasizing the role of thermal convection of moderately deep water.

ACKNOWLEDGMENTS

The authors thank M. Komatsu for his donation of Kuzuu samples to us, T. Ozawa for his advice on fusulinid fossil age and stratigraphic studies of Kuzuu area, and T. Tanaka for his advice and suggestion for Sr isotopic data. Critical comments by M. Minami were valuable in revising the earlier manuscript. This work was supported partly by the grants Nos. 03402018 and 06453007 from the Ministry of Education, Science and Culture, Japan to IK.

REFERENCES

Aharon, P., Socki, R.A. and Chan, L. (1987) Dolomitization of atolls by sea water convection flow: Test of a hypothesis at Niue, South Pacific. *Geology*, **95**, 187–203.

Anders, E. and Grevesse, N. (1989) Abundances of the elements: Meteoritic and solar. *Geochim. Cosmochim. Acta*, **53**, 197–214.

Ando, A., Okai, T., Inouchi, Y., Igarashi, T., Sudo, S., Marumo, K., Itoh, S. and Terashima, S. (1990) JLk-1, JLs-1 and JDo-1, GSJ rock reference samples of the "Sedimentary rock series". *Bull. Geol. Surv. Japan*, **41**(1), 27–48.

Asahara, Y., Tanaka, T., Kamioka, H., Nishimura, A. and Yamazaki, T. (1999) Provenance of the north Pacific sediments and process of source material transport as derived from Rb-Sr

isotopic systematics. *Chem. Geol.*, **158**, 271–291.

Banner, J.L., Hanson, G.N. and Meyers, W.J. (1988a) Rare earth element and Nd isotopic variations in regionally extensive dolomites from the Burlington-Keokuk Formation (Mississippian): Implications for REE mobility during carbonate diagenesis. *J. Sedimen. Petrol.*, **58**, 415–432.

Banner, J.L., Hanson, G.N. and Meyers, W.J. (1988b) Determination of initial Sr isotopic compositions of dolostones from the Burlington-Keokuk Formation (Mississippian): Constraints from cathodoluminescence, glauconite paragenesis and analytical methods. *J. Sedimen. Petrol.*, **58**, 673–687.

Bau, M., Koschinsky, A., Dulski, P. and Hein, J.R. (1996) Comparison of partitioning behaviors of yttrium, rare earth elements, and titanium between hydrogenetic ferromanganese crusts and seawater. *Geochim. Cosmochim. Acta*, **60**, 1709–1725.

Bellanca, A., Masetti, D. and Neri, R. (1997) Rare earth elements in limestone/marlstone couplets from the Albian-Cenomanian Cismon section (Venetian region, northern Italy): assessing REE sensitivity to environmental changes. *Chem. Geol.*, **141**, 141–152.

Bertram, C.J. and Elderfield, H. (1993) The geochemical balance of the rare earth elements and neodymium isotope in the oceans. *Geochim. Cosmochim. Acta*, **57**, 1957–1986.

Byrne, R.H. and Sholkovitz, E.R. (1996) Marine chemistry and geochemistry of the lanthanides. *Handbook on the Physics and Chemistry of Rare Earths*, (Gschneidner, K.A. and Eyring, L., eds.), vol. 23, 497–593, Elsevier Amsterdam.

Denison, R.E., Koepnick, R.B., Burke, W.H., Hetherington, E.A. and Fletcher A. (1994) Construction of the Mississippian Pennsylvanian and Permian seawater $^{87}Sr/^{86}Sr$ curve. *Chem. Geol.*, **112**, 145–167.

Flood, P.G., Fagerstrom, J.A. and Rougerie, F. (1996) Interpretation of the origin of massive replacive dolomite within atolls and submerged carbonate platforms: strontium isotopic signature ODP Hole 866A, Resolution Guyot, Mid-Pacific Mountains. *Sed. Geol.*, **101**, 9–13.

Fujinuki, T., Igarashi, T. and Hosogoe, C. (1982) Geochemical study of the Permian carbonate rocks form the Kuzuu district, Tochigi Prefecture, central Japan. *Bull. Geol. Surv. Japan*, **33**, 187–206.

German, C.R. and Elderfield, H. (1990) Rare earth elements in the NW Indian Ocean. *Geochim. Cosmochim. Acta*, **54**, 1929–1940.

German, C.R., Masuzawa, T., Greaves, M.J., Elderfield, H. and Edmond, J.M. (1995) Dissolved rare earth elements in the Southern Ocean: Cerium oxidation and the influence of hydrography. *Geochim. Cosmochim. Acta*, **59**, 1551–1558.

Harland, W.B., Armstrong, R.L., Cox, A.V., Craig, L.E., Smith, A.G. and Smith, D.G. (1990) A geologic time scale 1989. *Cambridge Univ. Press*

Igo, H. and Igo, H. (1977) Upper Permian fusulinaceans contained in the pebbles of the basal conglomerate of the Adoyama Formation, Kuzuu, Tochigi Prefecture, Japan. *Trans. Proc. Palaeont. Soc. Japan, N. S.*, **106**, 89–99.

Kawabe, I., Kitahara, Y. and Naito, K. (1991) Non-chondritic yttrium/holmium ratio and lanthanide tetrad effect observed in pre-Cenozoic limestones. *Geochem. J.*, **25**, 31–44.

Kawabe, I., Inoue, T. and Kitamura, S. (1994) Comparison of REE analyses of GSJ carbonate rocks by ICP-AES and INAA: Fission and spectral interferences in INAA determination of REE in geochemical samples with high U/REE ratios. *Geochem. J.*, **28**, 19–29.

Kawabe, I., Toriumi, T., Ohta, A. and Miura, N. (1998) Monoisotopic REE abundances in seawater and the origin of seawater tetrad effect. *Geochem. J.*, **32**, 213–229.

Kawabe, I., Ohta, A. and Miura, N. (1999) Distribution coefficients of REE between Fe oxyhydroxide precipitates and NaCl solutions affected by REE-carbonate complexation. *Geochem. J.*, **33**, 181–197.

Kobayashi, F. (1979) Petrography and sedimentary environment of the Permian Nabeyama limestone in the Kuzuu area, Tochigi Prefecture, central Japan. *J. Geol. Soc. Japan*, **85**, 627–642.

Ludwig, K.R., Halley, R.B., Simmons, K.R. and Peterman, Z.E. (1988) Strontium-isotope stratigraphy of Enewetak Atoll. *Geology*, **16**, 173–177.

Matsuda, H. and Iijima, A. (1989) Occurrence and genesis of Permian dolostone in the Kuzuu area,

Tochigi Prefecture, central Japan. *Jour. Fac. Sci. Univ. Tokyo section II*, **22**, 89–119.

Mazumdar, A., Tanaka, K., Takahashi, T. and Kawabe, I. (2003) Characteristics of rare earth element abundances in shallow marine continental platform carbonates of Late Neoproterozoic successions from India. *Geochem. J.*, **37**, 277–289.

Miura, N. and Kawabe, I. (2000) Dolomitization of limestone with $MgCl_2$ solution at 150°C: Preserved original signatures of rare earth elements and yttrium as marine limestone. *Geochem. J.*, **34**, 223–227.

Mountjoy, E.W., Qing, H. and McNutt, R.H. (1992) Strontium isotopic composition of Devonian dolomites, Western Canada Sedimentary Basin: significance of sources of dolomitizing fluids. *Appl. Geochem.*, **7**, 59–75.

Ohde, S. and Elderfield, H. (1992) Strontium isotope stratigraphy of Kita-daito-jima Atoll, North Philippine Sea: implications for Neogene sea-level change and tectonic history. *Earth Planet. Sci. Lett.*, **113**, 473–486.

Ohta, A., Ishii, S., Sakakibara, M., Mizuno, A. and Kawabe, I. (1999) Systematic correlation of the Ce anomaly with the Co/(Ni+Cu) ratio and Y fractionation from Ho in distinct types of Pacific deep-sea nodules. *Geochem. J.*, **33**, 399–417.

Palmer, M.R. and Edmond, J.M. (1989) The strontium isotope budget of the modern ocean. *Earth Planet. Sci. Lett.*, **92**, 11–26.

Piepgras, D. and Jacobsen, S.B. (1992) The behavior of rare earth elements in seawater: Precise determination of variations in the North Pacific water column. *Geochim. Cosmochim. Acta*, **56**, 1851–1862.

Quing, H. and Mountjoy, E.W. (1994) Rare earth element geochemistry of dolomites in the Middle Devonian Presquile barrier, Western Canada Sedimentary Basin: implications for fluid-rock ratios during dolomitization. *Sedimentology*, **41**, 787–804.

Rodgers, K.A., Easton, A.J. and Downes, C.J. (1982) The chemistry of carbonate rocks of Niue Island, South Pacific. *Jour. Geol.*, **90**, 645–662.

Saller, A.H. and Koepnick, R.B. (1990) Eocene to early Miocene growth of Enewetak Atoll: Insight from strontium-isotope data. *Geol. Soci. Am. Bull.*, **102**, 381–390.

Sano, H. and Kanmera, K. (1988) Paleogeographic reconstruction of accreted oceanic rocks, Akiyoshi, southwest Japan. *Geology*, **16**, 600–603.

Schofield, J.C. and Nelson, C.S. (1978) Dolomitization and Quaternary climate of Niue Island, Pacific Ocean. *Pacific. Geol.*, **13**, 37–48.

Shaw, H.F. and Wasserburg, G.J. (1985) Sm-Nd in marine carbonates and phosphates: implications for Nd isotopes in seawater and crust ages. *Geochim. Cosmochim. Acta*, **49**, 503–518.

Sholkovitz, E., Landing, W.M. and Lewis, B.L. (1994) Ocean particle chemistry: The fractionation of rare earth elements between suspended particles and seawater. *Geochim. Cosmochim. Acta*, **58**, 1567–1579.

Sholkovitz, E. and Shen, G.T. (1995) The incorporation of rare earth elements in modern coral. *Geochim. Cosmochim. Acta*, **59**, 2749–2756.

Tanaka, K., Ohta, A. and Kawabe, I. (2004) Experimental REE partitioning between calcite and aqueous solution at 25°C and 1 atm: Constraints on the incorporation of seawater REE into seamount-type limestones. *Geochem. J.*, **38**, 19–32.

Tanaka, K., Miura, N., Asahara, Y. and Kawabe, I. (2003) Rare earth and strontium isotopic study of seemount-type limestones in Mesozoic accretionary complex of Southern Chichibu Terrane, central Japan: Implication for incorporation process of seawater REE into limestones. *Geochem. J.*, **37**, 163–180.

Webb, G.E. and Kamber, B.S. (2000) Rare earth elements in Holocene reefal microbialites: A new shallow seawater proxy. *Geochim. Cosmochim. Acta*, **64**, 1557–1565.

Yanagimoto, H. (1973) Stratigraphy and geological structure of the Paleozoic and Mesozoic formations in the vicinity of Kuzuu, Tochigi Prefecture. *Bull. Geol. Soc. Japan*, **79**, 441–451.

Zhang, J., Amakawa, H. and Nozaki, Y. (1994) The comparative behaviors of yttrium and lanthanides in the seawater of the North Pacific. *Geochim. Cosmochim. Acta*, **60**, 4631–4644.

Zhang, J. and Nozaki, Y. (1996) Rare earth elements and yttrium in seawater: ICP-MS determinations in the East Caroline, Coral Sea, and South Fiji basins of the western South Pacific Ocean.

Geophys. Res. Lett., **21**, 2677–2680.

Zhong, S. and Mucci, A. (1995) Partitioning of rare earth elements (REEs) between calcite and seawater solutions at 25°C and 1 atm, and high dissolved REE concentrations. *Geochim. Cosmochim. Acta*, **59**, 443–453.